A Wavelet-based Filtering Algorithm for Enhancing Signal Processing in Coriolis Flow Meters

David Wee Yang Khoo[1*], *Zhi Qun* Ng[2], and *Leong Keey* Seah[2]

[1]National Metrology Centre, Agency for Science and Technology Research, Singapore
[2]Nanyang Technological University, Singapore

Abstract. Applying signal processing method effectively for a Coriolis flow meter (CFM) requires robust filtering strategies. This is because in actual bunkering processes, various noise components can be generated resulting in unreliable mass flow rate measurements. This study introduces a wavelet transform-based filtering algorithm to denoise and extract relevant features from non-stationary signals. It can be observed that the db6 and sym6 wavelets, with SURE and FDR thresholding, achieve the highest SNR values and lowest RMSE. The sym6 wavelet & SURE threshold exhibited good noise reduction effect and were used for further analysis. It was also found that FFT with Zero Padding paired with Wavelet Denoising & Cross Correlation yielded a percentage error of < 1% when comparing with the original simulated signal.

1 Introduction

CFMs are widely used in the oil and gas industries, from upstream allocation to downstream bunkering and transmission pipeline custody transfer. Since 2017, the Maritime and Port Authority (MPA) has mandated the use of CFMs for ship-to-ship fuel oil custody transfers under Singapore Standard (SS) 648 (or ISO 22192) [1]. The CFM operates on the Coriolis force principle and comes in various designs, including straight-tube, S-shape, and V-shape [2]. In a U-shaped CFM, a driver excites the tube at its resonant frequency, causing fluid momentum and oscillatory motion to induce a Coriolis force, which results in a phase shift along the tube's length as shown in Figure 1.

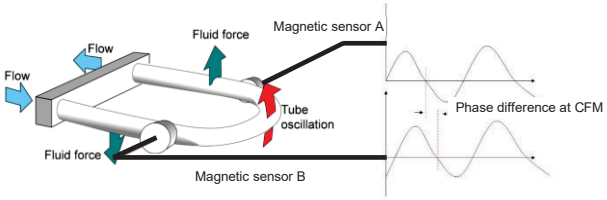

Figure 1: Schematic diagram of a U-shape CFM and the pickup sensors signal profiles with their corresponding phase difference.

The phase difference is then used to calculate the time delay and determine the mass flow rate [3]. Reliable determination of the phase difference is hence critical for measuring the mass flow rate accurately especially for high-precision applications. There are a few ways to improve the accuracy of the mass flow rates measured by a CFM. One of the methods involves AI techniques such as Long Short-Term Memory and Support Vector Machine that make use of sensor signals as sample characteristics to relate sensor signals to mass flow rate, but these algorithms can be time-intensive and difficult to interpret. Another method is to theoretically derive a solution and apply signal processing methods to develop an algorithm with high robustness and anti-interference capabilities. However, to apply the signal processing method effectively requires robust filtering strategies. This is because in actual bunkering processes, various noise components can be generated resulting in unreliable mass flow rate measurements. For annual bunker sales of 50 million tonnes, a small error of 0.1% may potentially cause a loss of approximately ~50,000 tonnes or US$25 million if a price $500/ton of bunker oil loaded in fuelling ships. External noise and vibrations are natural occurrences in the bunkering process and can affect CMF accuracy, making it challenging to extract reliable phase components [4]. Noise can come from sources like pumps, nearby equipment, or turbulence in the fluid, all of which can interfere with the vibrating tube of CMF and reduce measurement accuracy. As such, effective filtering techniques are required to remove the unwanted noise components while extracting reliable phase components information. Common filtering techniques include Moving Average, FIR/IIR Filters, Adaptive Notch Filters (ANF), Windowing Functions and Hilbert Transform [3-5].

Frequency-domain filtering like Window Functions often encounter spectral leakage where the truncation of signals and non-integer sampling rates distort the signals especially when using window functions with significant sidelobes. These sidelobes can lead to "ringing" effects which are unwanted oscillations or

* Corresponding author: david_khoo@nmc.a-star.edu.sg

ripples at the edges of the signals where the windows tapers off. In contrast, time-domain filtering is generally more effective at handling non-stationary signals and can mitigate some of the spectral leakage issues associated with frequency-domain filtering. However, its performance depends heavily on the noise characteristics and may also distort high frequency components. Therefore, selecting an appropriate filtering technique is imperative to accurately extract phase difference information in the presence of noise to ensure more reliable mass flow measurements.

To address this challenge, this work aims to develop a reliable filtering algorithm based on wavelet transform to suppress the noise interference generated during the bunkering process. Wavelet transforms were utilised to denoise the signals and extract relevant features, particularly in cases involving non-stationary signals or transient noise. This study analysed the impact of different wavelet functions and thresholding methods across various levels of decomposition on the filtering of simulated signals used in mass flow rate calculations. Cross-correlation was used to estimate the phase shift between the two sensor signals for the determination of mass flow rates.

2 Methodology Development

2.1 Numerical Signals and Boundary Conditions

A time-varying signal model, where the signal's frequency, amplitude, and phase change based on a random walk model [3] has been developed to represent CMF signals.

$$y_1(n) = A(n)\,sin\left[\omega(n) + \phi_{\,1}(n)\right] \cdot dt + e_1\,(n) \quad (1)$$

$$y_2(n) = A(n)\,sin\left[\omega(n) + \phi_{\,2}(n)\right] \cdot dt + e_2\,(n) \quad (2)$$

$$A(n) = A(n-1) + \delta_A \cdot \sigma_A \cdot e_A(n) \quad (3)$$

$$\omega(n) = \omega(n-1) + \delta_\omega \cdot \sigma_\omega \cdot e_\omega(n) \quad (4)$$

$$\phi(n) = \phi(n-1) + \delta_\phi \cdot \sigma_\phi \cdot e_\phi(n) \quad (5)$$

Where y_1 and y_2 are simulated sensor signals with amplitude A, angular frequency ω, phase lag ϕ and time step dt, $dt=1/f_s$. $e_1(n)$, $e_2(n)$, $e_A(n)$, $e_\omega(n)$, $e_\phi(n)$ are white noise following a Gaussian distribution and has no correlation with one another. δ_A,δ_ω and δ_ϕ are binary walk factors (0 – 1) with probabilities P_A, P_ω *and* P_ϕ [3]. Table 1 shows the boundary conditions of the parameter used for simulating the sensor signals. Figure 2 demonstrates the simulated signal and its corresponding frequency and phase difference profiles.

Table 1: Initialisations of signal parameters

Name	Initial Value
Amplitude	$A(0) = 5\text{mV}$
Frequency	$f = 105Hz$
Probabilities	$P_A = P_\omega = P_\phi = 0.5$
Sample frequency	$f_s = 2000Hz$
Step size	$\sigma_A = 10^{-4}$, $\sigma_\omega = 10^{-6}$, $\sigma_\phi = 10^{-4}$

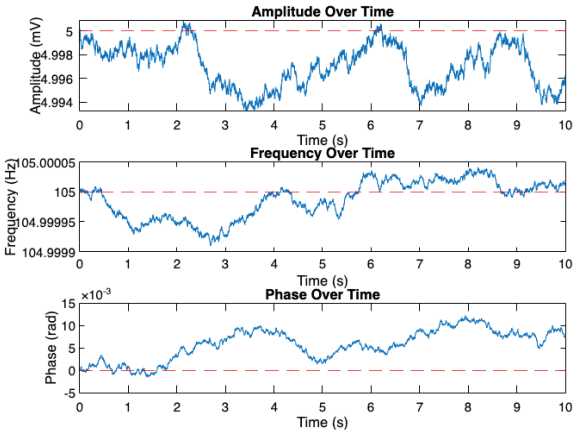

Figure 2: Simulated signal time domain plots

2.2 Wavelet Denoising

Noise reduction is a critical step in signal processing to improve the accuracy and reliability of measured data. Wavelet denoising leverages the ability of the Discrete Wavelet Transform (DWT) to separate a signal into frequency components at varying resolutions. This approach assumes that noise predominantly affects high-frequency components, while the key features of the signal are concentrated in the low-frequency components.

2.2.1 Wavelet Decomposition

The DWT decomposes a signal into wavelet coefficients, which represent the signal's approximation (low-frequency) and detail (high-frequency) components at multiple levels of resolution as illustrated in Figure 3.

The mathematical representation of the DWT is:

$$\alpha_{j,k} = \sum_n x[n]\phi_{j,k}[n] \quad (6)$$

$$d_{j,k} = \sum_n x[n]\psi_{j,k}[n] \quad (7)$$

Where, $\alpha_{j,k}$ represents the Approximation Coefficients and $d_{j,k}$ the Detail Coefficients. j is the level of decomposition, k is the position in time, $\phi_{j,k}[n]$ is the scaling function and $\psi_{j,k}[n]$ is the type of wavelet. The choice of wavelet function is critical, as it influences the effectiveness of the decomposition. Selecting an appropriate wavelet that aligns with the characteristics of the signal can significantly enhance the decomposition process, leading to a more precise separation between the signal and noise components. Factors such as symmetry, regularity, and support width determine a wavelet's suitability for a given signal [6]. In this study, wavelets such as Haar, Daubechies (db6), and Symlets (sym6) were evaluated for their performance in separating noise from signal components.

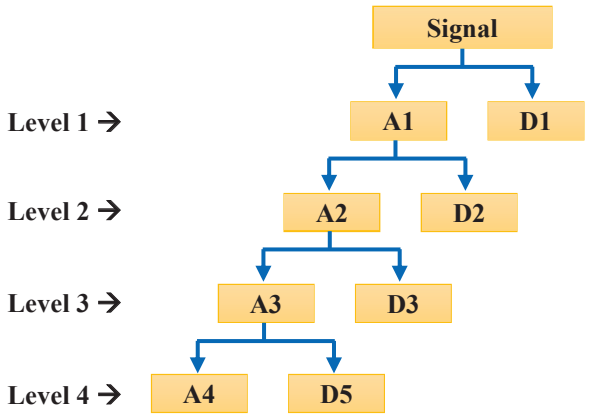

Figure 3: Wavelet Decomposition Tree

2.2.2 Thresholding Techniques

After decomposition, noise reduction is achieved by applying thresholding to the detail coefficients. By setting small coefficients—often attributed to noise—to zero or shrinking them toward zero, we can suppress noise while retaining the underlying signal structure. [6]. In this work, several thresholding techniques were assessed for wavelet denoising, such as the Universal threshold, SURE (Stein's Unbiased Risk Estimate), Minimax threshold, and False Discovery Rate (FDR). After thresholding, the signal is then reconstructed from the modified coefficients using the Inverse Discrete Wavelet Transform (IDWT). The reconstruction process also depends on both the selected wavelet function and the type of thresholding, ensuring that the key features of the actual signal are preserved with minimal distortion. This step combines the thresholder detail coefficients with the approximation coefficients to produce the denoised signal.

2.3 Phase Difference Extraction

Cross-correlation was used to determine the time delay by measuring signal similarity. By shifting one signal relative to the other and computing their pointwise product, the cross-correlation function identifies the time lag at which the signals align most closely. The cross-correlation between two time-domain signals $x(t)$ and $y(t)$ is defined as:

$$R_{xy}(\tau) = \int_{-\infty}^{\infty} x(t)y(t+\tau)dt \tag{8}$$

Where τ represents the time lag. For discrete signals, the formula becomes:

$$R_{xy}[k] = \sum_{n=0}^{N-1} x[n]y[n+k] \tag{9}$$

Where k is the discrete time lag (in samples) and N represents the length of the signal. To compute the cross-correlation for discrete signals, the process iterates over all possible lag values of k. Starting with $k = 0$, the two signals are aligned without any shift and their pointwise product is computed and summed. The iterative process continues for all positive and negative lag values, evaluating the similarity of the signals at each shift. At the highest R_{xy} value, the corresponding lag, k_{max} was extracted and calculate the phase shift (in degrees) $\Delta\,\theta = \frac{k_{max}}{fs} * 360 * f$.

3 Results and Discussion

Two performance indicators namely: Signal-to-Noise Ratio (SNR) and Root Mean Square Error (RMSE), were used to assess the precision and dependability of the wavelets. The SNR was selected as a performance metric because it measures the strength of the desired signal relative to the background noise. RMSE offers an interpretation of the units of the target variable. The SNR and RMSE formulations are as follows:

$$SNR = 10 \cdot \log\left(\frac{\sum_{n=1}^{N} f(n)^2}{\sum_{n=1}^{N}\left(f(n) - \hat{f}\right)}\right)^2 \tag{10}$$

$$RMSE = \sqrt{\frac{1}{N}\sum_{n=1}^{N}\left(f(n) - \hat{f}(n)\right)^2} \tag{11}$$

Where n is the number of test samples, $f(n)$ is the noise containing signal and $\hat{f}(n)$ is the signal after denoising. Figure 4 (a) illustrates the results of wavelet denoising using the haar wavelet with different types of thresholding. The blue signal represents the reconstructed signal after denoising, while the green signal represents the true signal. Ideally, if the blue signal closely matches the shape of the green signal, it will indicate high accuracy in the denoising process. A perfect match between the two signals would signify 100% accuracy in removing noise without distorting the underlying signal. Figures 4 (b) & (c) compare the performance of different wavelets and thresholding methods. It can be found that the db6 and sym6 wavelets, when used with SURE and FDR thresholding, achieve the highest SNR values. Additionally, these wavelets exhibit the lowest RMSE, indicating superior denoising performance compared to other combinations. The results are also consolidated and shown in Table 2.

The combination of the sym6 wavelet with SURE thresholding consistently produced the best denoising results for the sinusoidal signals in this study. While other thresholding methods, such as universal or minimax, tend to be more conservative and thus oversmoothed the signal, SURE adaptively selects a threshold that preserves essential signal features. At the same time, the sym6 wavelet which is designed to be nearly symmetric, exhibit approximately linear phase behaviour. This ensures that the reconstructed signal maintains its original phase alignment, preventing unwanted shifts. Moreover, sym6 has 6 vanishing moments, allowing it to efficiently represent

polynomials of up to degree 5. Since sym6 can accurately model smooth, oscillatory behaviour like sinusoidal signals, it enhances the separation of signal-containing coefficients from noise-containing coefficients. This improved distinction allows for thresholding to be more effective. Making it easier to eliminate noise while preserving the signal components.

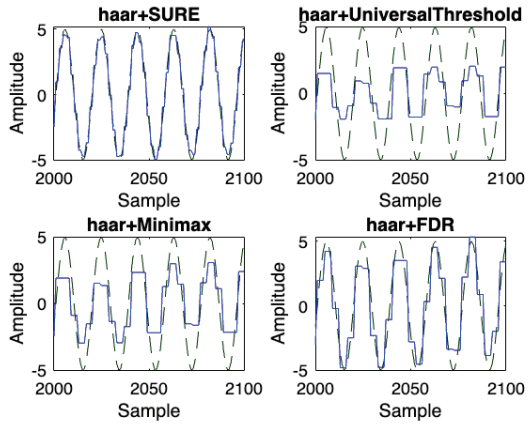

(a)

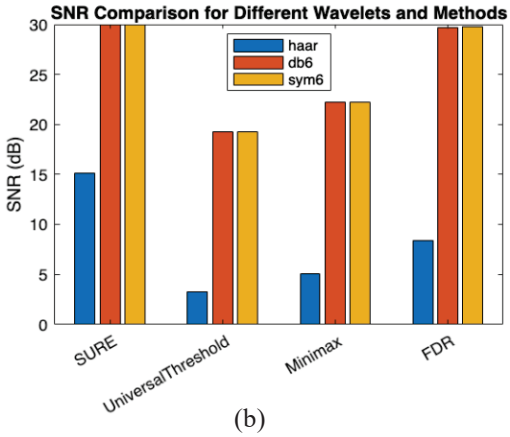

(b)

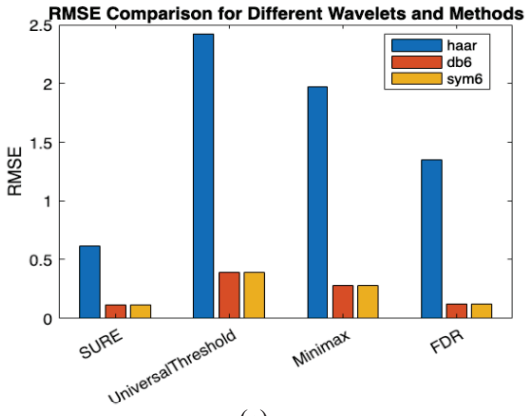

(c)

Figure 4: (a) Thresholding variations for haar wavelets, and the performance assessment for different wavelets and thresholding methods based on (b) SNR and (c) RMSE.

Table 2: Initialisations of signal parameters

Wavelet	Threshold Value	SNR	RMSE (mV)	Ranking
Sym 6	SURE	29.8624	0.1136	1
	Universal Threshold	18.9562	0.3987	4
	Minimax	21.8613	0.2854	3
	FDR	29.6268	0.1167	2

The combination of sym6 wavelet & SURE threshold exhibited good noise reduction effect and were used to obtain the phase difference using Cross Correlation. It was also found FFT with Zero Padding paired with Wavelet Denoising & Cross Correlation yielded a percentage error of < 1% when comparing with the pre-assigned boundary condition.

4 Conclusion and Future Work

The sym6 wavelet and SURE threshold effectively reduced noise and were used for further analysis. FFT with Zero Padding, combined with Wavelet Denoising and Cross Correlation resulted in a percentage error of < 1% compared to the pre-assigned sensor signal. A graphical user interface was created based on the designed numerical model and will be validated with experimental work for different mass flow conditions using the NMC liquid flow facility in the next stage of this research work.

References

1. SS 648 : 2019, Code of practice for bunker mass flow metering, Singapore Standards Council.
2. C. Tan, F. Dong, “Sensor instrumentation for flow measurement.”, Encyclopedia of Sensors and Biosensors, vol. 3, pp. 536-554, 2023.
3. Y. Tu, H. Yang, H. Zhang, X. Liu “CMF signal processing method based on feedback corrected ANF and hilbert transformation.” Measurement Science Review, vol. 14, 2014.
4. N. Chen, “Research on coriolis mass flowmeter filtering algorithm based on MALLAT algorithm.” ICFTIC, pp. 861-865, 2023
5. M. Li, M. Henry, “Signal processing methods for coriolis mass flow metering in two-phase flow conditions.” IEEE ICIT, pp. 690-695, 2016.
6. F. Xiao and Y. Zhang, “A comparative study on thresholding methods in wavelet-based image denoising.” Procedia Engineering, vol. 15, pp. 3998–4003, 2011.

Acknowledgements

This research work was supported by the Agency for Science, Technology and Research (A*STAR) - Career Development Fund (CDF), <C233312022>.